GEOPHYSICAL RESEARCH LETTERS, VOL. 23, NO. 1, PAGES 109-112, JANUARY 1, 1996

Phase coupling in Langmuir wave packets: Possible evidence of three-wave interactions in the upstream solar wind

S. D. Bale and D. Burgess

Astronomy Unit, Queen Mary and Westfield College, London, United Kingdom

P. J. Kellogg, K. Goetz, R. L. Howard and S. J. Monson

School of Physics and Astronomy, University of Minnesota, Minneapolis

Abstract. Some theories of the generation of $2\omega_{pe}$ radiation, in the upstream solar wind, invoke the notion of nonlinear wave-wave interactions. We present observations, from the WIND spacecraft, of an event in the upstream solar wind with first and second harmonic emissions. The bicoherence spectrum of this event shows coherence amongst components that suggest three-wave interactions of the type described in (Cairns and Melrose, 1985). We discuss this result and its theoretical context.

Introduction

Electromagnetic emission at the second harmonic of the local electron plasma frequency is well documented in the upstream solar wind [*Dunckel*, 1974; *Gurnett*, 1975] and associated with solar type-III bursts [*Wild et al.*, 1963]. The theoretical framework of such emission is generally considered to be that of nonlinear wave-wave interactions. In particular, a mechanism whereby transverse waves at $2\omega_{pe}$ are generated by the coalescence of two Langmuir waves $L + L' \rightarrow T$ has been put forth [*Ginzburg and Zheleznyakov*, 1958; *Cairns and Melrose*, 1985]. With this thesis, a primary spectrum of Langmuir waves is generated by a beam instability. This primary spectrum undergoes decay or coalescence with existing ion acoustic turbulence such that $L \pm S \rightarrow L'$ and a secondary spectrum of 'backward' Langmuir waves is generated. These two distributions then coalesce to give $L + L' \rightarrow T$: transverse waves at roughly twice the local plasma frequency. A necessary condition of the final interaction is the phase coherence of the two Langmuir waves with the resulting electromagnetic wave. In this letter we present the bicoherence spectrum of time domain electric field data showing $2\omega_{pe}$ radiation. This bicoherence exhibits peaks which correspond to the $L + L' \rightarrow T$ reaction. The bicoherence measures the degree to which the frequency components are phase coupled, and hence, related quadratically.

Paper number 95GL03595
0094-8534/96/95GL-03595$03.00

Experiment

The WIND spacecraft was launched on 1 November, 1994 and made a series of Earth orbits in late 1994. Between launch and 26 December, 1994, there were 8 crossings of the Earth's bow shock. WIND crossed the shock at roughly 12:00 UT on 12 December; this data is taken in the foreshock region upstream of the shock, before the crossing, on that day.

The data presented here are from the Time Domain Sampler (TDS) experiment of the WAVES instrument. The TDS samples various combinations of the electric field antennas and search coil magnetometers at sample speeds up to 120,000 samples per second. The sampled signal is returned as a signed logarithm allowing for 90 dB of dynamic range from threshold values near 80 μV (RMS). The high speed channels of the TDS (Channels 1 and 2) can be connected, at various times, to the E_x, E_y, or E_z antennas. The X and Y antennas are simple wire dipoles in the spin plane with lengths of 100 and 15 meters tip-to-tip, respectively. The Z axis antenna, a rigid dipole, is along the spin axis with a length of about 5 meters tip-to-tip. For the data interval shown here, TDS channels 1 and 2 were connected to the E_x and E_z antennas and sampling at 120,000 samples per second with a low pass filter above 50 kHz to reduce frequency aliasing. The TDS experiment samples waveforms continuously and, based on a predetermined quality, returns the largest events with the peak amplitude centered in an interval of 2048 points. The E_z signal, not shown here, is much weaker and suffers corruption near the instrument zero. It is, therefore, less useful for detailed analysis but shows the same general features as the E_x signal presented below. More details of this instrument are described in [*Bougeret et al.*, 1995].

Bispectral Analysis

The classical bispectrum measures the degree of phase coupling between the frequency components of a signal such that $\omega_1 + \omega_2 = \omega_3$ where $\omega_3 < \omega_{Nyquist}$. Defined as $B(\omega_1, \omega_2) = \langle X(\omega_1) X(\omega_2) X^*(\omega_1 + \omega_2) \rangle$, it is the spectral transform of the third moment sequence of $x(t)$, and as such gives indication of quadratic coupling

of the modes of the system [*Kim and Powers*, 1979]. The angle brackets denote an ensemble average. The bicoherence is the normalized amplitude [*Kravtchenko-Berejnoi*, 1994] of the bispectrum,

$$b^2(\omega_1,\omega_2) = \frac{|B(\omega_1,\omega_2)|^2}{\langle |X(\omega_1)||X(\omega_2)||X^*(\omega_1+\omega_2)|\rangle^2} \quad (1)$$

and takes a value $b^2 \in \{0,1\}$. The bicoherence has maxima at frequency pairs which are phase related as $\phi(\omega_1,\omega_2) = \phi(\omega_1)+\phi(\omega_2)-\phi(\omega_1+\omega_2)+\phi_0$ and is zero in the presence of randomly phased Gaussian noise. Bispectral analysis has been applied successfully to data from both laboratory experiments [*Kim and Powers*, 1979] and space plasma experiments [*Lagoutte et al.*, 1989; *Labelle and Lund*, 1992; *Dudok de Wit and Krasnosel'skikh*, 1995] and appears to be a useful tool in the diagnosis of nonlinear plasma processes.

In this work, we use the bicoherence calculated from the imaginary part of the bispectrum. [*Elgar*, 1987] shows that the imaginary part of the bispectrum is more sensitive to the time evolution of the signal while the real part is sensitive to the vertical asymmetry. While large amplitude variations are indeed part of the spectral structure of the signal, finite ensemble size allows fewer samples at these frequencies and, therefore, more error due to nonstationarity. Langmuir waves are inherently bursty and this is done, in part, to address the nonstationarity of the data. Most spectral analysis methods assume some stationarity of the data; in particular, the bispectrum is ideally calculated on a stationary wave spectrum. We have treated the data as a set of overlapping ensembles to improve the statistics but the results may still be adversely affected by the time development of the waveform. For future work we may implement a wavelet bicoherence algorithm [e.g. *Dudok de Wit and Krasnosel'skikh*, 1995]. Another effect to consider is Doppler shift. While the phase coupling should be frame invariant, the bispectrum does require that the participating modes be confined to the Nyquist interval; waves participating in a interaction, but unsampled or undersampled, would not generate reliable bicoherence.

Results

Near 01:00 UT 12 December 1994, WIND was roughly 17 R_e radially upstream of the bow shock. The shock crossing, inferred from key parameter (46 second averaged) magnetic field data, was near 12:00 UT at 10 R_e near the subsolar point. These average magnetic field data show a low level of fluctuations before roughly 08:00 UT, implying that the spacecraft was not yet in the ion foreshock region. Additionally, the thermal noise receiver (TNR) instrument shows the presence of $2\omega_{pe}$ radiation. The spacecraft was near the solar wind-electron foreshock boundary and made several passes through this region of intense Langmuir wave activity.

Figure 1 shows a TDS Channel 1 event on 01:09:48 UT, 12 December 1994 and its wavelet spectrum. The wavelet spectrogram is calculated with a Morlet wavelet [*Goupillaud et al.*, 1984; *Lagoutte et al.*, 1992]. Essentially, a Gaussian profile wavelet, $g(t) = e^{i\omega_0 t}e^{-t^2/2}$, is convolved with the electric field signal and dilated to yield frequency components. This is a local spectral representation and its spectrogram, although somewhat computationally demanding, gives more information in the time domain than a standard Fourier spectrogram.

The Langmuir waves in Figure 1 are very bursty and modulated by a lower frequency component. The power spectrum (Figure 2) of the entire event shows two large components near the local plasma frequency and some smaller peaks at and around the second harmonics. The low pass filtering above 50 kHz reduces the measured amplitude of the second harmonic features. It can be seen from the wavelet spectrum that the region of strong low frequency modulation, between roughly 7.5 and 10 milliseconds, corresponds to the temporal overlap of the two frequency components near the local ω_{pe} ($\sim 25-30kHz$). Any quadratic interaction of the two waves should produce waves at both the sum and difference frequencies. Indeed, the frequency of the low frequency modulation between 7.5 and 10 milliseconds corresponds roughly to the difference frequency between the ω_{pe} peaks. Some substructure is visible in the main peaks of the power spectrum. In particular, there are $\sim 500Hz$ up- and down-shifted subpeaks.

The top panel of Figure 2 shows the normalized imaginary bicoherence of the E_x data. This bispectrum is

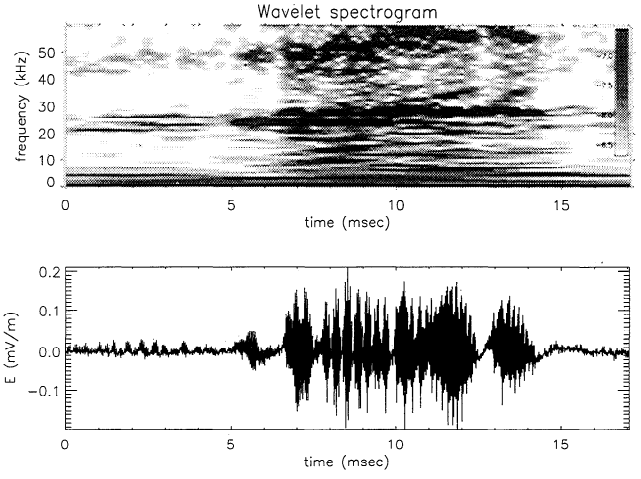

Figure 1. TDS electric field measurement, from the X antenna, and its wavelet spectrogram. A slight rise in the wave frequency occurs over this interval. Between 7.5 and 10 milliseconds, the two regimes of plasma waves appear to be beating together and forming sidebands. Second harmonic emission is visible during the most intense wave activity. The greyscale is logarithmic spanning roughly two orders of magnitude of power, in arbitrary units. In the spectrogram, there are 64 frequency bins with $\delta f/f \sim 1/24$.

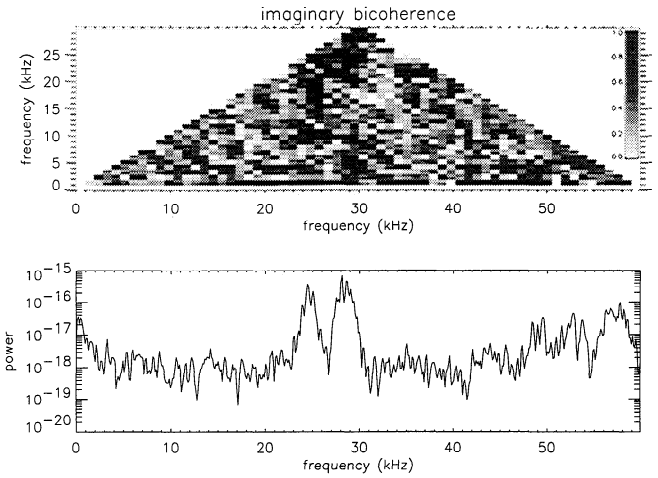

Figure 2. Fourier power spectrum and imaginary bicoherence. The two peaks on the power spectrum correspond to the early and later values of the local plasma frequency. Large values of bicoherence at $(\omega_1, \omega_2) \sim (24.5, 24.5)$ kHz and $(\omega_1, \omega_2) \sim (29, 29)$ kHz, imply that these components interact to produce the power at 49 kHz and 58 kHz, respectively. A large bicoherence at $(\omega_1, \omega_2) \sim (24.5, 29)$ kHz is evidence of the interaction of the two plasma frequency components to produce the peak near 53 kHz. The statistical significance of the bicoherence is discussed in the text.

calculated using overlapping ensembles of Fourier transforms of the data in Figure 1. The bicoherence is then calculated, as in equation (1), using the imaginary part of the bispectrum. As mentioned above, this highlights coupled modes which contribute to the time development (fore-aft asymmetry) of the waveform. A method recently put forth by [*Dudok de Wit and Krasnosel'skikh*, 1995] uses Morlet wavelet transforms as the spectral estimators for the bispectrum and we may implement it for later work. The bicoherence, as mentioned above, measures the degree of phase coupling between frequency components; as such, it indicates a quadratic nonlinearity amongst frequency components. The theory of weak plasma turbulence [e.g. *Melrose*, 1980] is formulated in terms of a quadratic current which is an integral of interacting wave fields over a nonlinear response tensor. Hence, weak three-wave interactions necessarily involve phase coupled fields and should appear strongly on a bicoherence spectrum as points in the (ω_1, ω_2) plane where the waves are coupled as $\omega_1 + \omega_2 = \omega_3$. Weak turbulence calculations are typically made in the random phase approximation (RPA) [*Melrose*, 1980]; this may be thought of as a computational aid that assumes no phase coherence between the input waves. It seems, however, that the output waves must be phase-coupled to the input waves given the quadratic nature of the interaction. So, while the individual wave triads must be phase-coupled, the RPA assumes that each triad is uncoupled from the background distribution.

The bicoherence in Figure 2 shows a few important features. There are peaks at $(\omega_1, \omega_2) =$ (24.5 kHz, 24.5 kHz), and $(\omega_1, \omega_2) =$ (29 kHz, 29 kHz). These peaks correspond to the process $L + L' \rightarrow T$ within each region of Langmuir waves and produce their respective second harmonics, as seen on the power spectrum. A peak near $(\omega_1, \omega_2) =$ (24.5 kHz, 29 kHz) is consistent with the process $L + L' \rightarrow T$ operating between the Langmuir waves with slightly different frequencies. This would be associated with the feature near 53 kHz on the power spectrum. A smaller peak near $(\omega_1, \omega_2) =$ (29 kHz, 3 kHz) may correspond to the difference wave from the (24.5 kHz, 29 kHz) process. There is no obvious mode here, though, and the feature does not appear on the power spectrum. There are significant peaks at lower frequencies in the real part of the bicoherence. These peaks are more susceptible to the finite record size, however, and while they could indicate the $L \pm S \rightarrow L'$ process, we don't attempt to interpret them. Here we concentrate on the higher frequency processes.

The statistical variance of the bicoherence is given by *Kim and Powers* [1979] to be $(1 - b^2(\omega_1, \omega_2))/M$ where M is the number of ensembles (16 in our case); hence, the larger peaks on the bicoherence are the most statistically reliable. The variance from the set of ensembles has also been calculated explicitly for the bicoherence and the peaks discussed above all show variance of about 0.1 - 0.15 and the values are locally minimum in the variance spectrum. These variances are larger that the theoretical variance by about a factor of 10. This is most likely the result of the nonstationary waveform; the bicoherence is significant when the two waves overlap and interact. The theoretical variance estimate of *Kim and Powers* [1979] assumes the stationarity of the power spectrum and long data records. Since these peaks have average bicoherence values near 1.0, it may be that some few ensembles have very small bicoherence in these bins. It is possible that instrumental effects produce the coupling. This, however, seems somewhat unlikely especially in the case of the peak at (ω_1, ω_2) = (24.5 kHz, 29 kHz) where the two separate carrier frequencies are coupled.

Conclusions

We have shown that waves in the upstream solar wind, near the local plasma frequency and second harmonic, are phase coupled as would be expected if the second harmonic were generated by the weak plasma turbulence process $L + L' \rightarrow T$. The power spectrum shows that Langmuir waves with two separate frequencies are present and that their frequency difference is ion acoustic-like; this difference frequency is weakly phase coupled to the Langmuir waves as well. This could be an indication of the process $L \pm S \rightarrow L'$, creating a secondary Langmuir wave population by interacting with ion acoustic waves, although no large S wave field is observed in our data. This reaction is but one step in

the scenario proposed by [*Cairns and Melrose*, 1985] as a possible mechanism of second harmonic generation. Langmuir 'beat' waveforms have been discussed in the context of the decay process $L \rightarrow L' + S$ alone by *Cairns and Robinson* [1992]. Our bispectral signature, however, clearly shows coupling for the second harmonic process. It must be noted that this analysis does not determine the direction of the arrow of three-wave processes. In particular, it could be the case that the second harmonic is generated by another mechanism and decays to two Langmuir waves.

It is not obvious what would be the bispectral signature of the alternative generation mechanisms. Both the strong turbulence schemes [*Papadopoulos et al.*, 1974] and the electrostatic quasi-mode model [*Yoon et al.*, 1994] may exhibit phase coupled fields. The formulation of the bispectrum [*Kim and Powers*, 1979] is ideal for detecting three-wave processes and we only show consistency with the weak turbulence models.

The event analyzed here is of relatively low amplitude. The WIND dataset includes hundreds of similar events in the upstream region, showing various bispectral signatures. Stronger events show a slightly different bispectrum, possibly due to a modulational instability, and this may be a topic of future work.

Acknowledgments. We would like to acknowledge enlightening discussions with S. J. Schwartz, T. Dudok de Wit, and V. V. Krasnosel'skikh. The WAVES instrument on WIND was built by teams at NASA GSFC, Observatoire de Paris, Meudon and the University of Minnesota. M.L. Kaiser is the Principal Investigator; J.-L. Bougeret is the Deputy PI. Use of the key parameter MFI data is courtesy of the Magnetic Fields Instrument data processing team and the ISTP CDHF team at NASA GSFC. This work was supported in part by PPARC (UK) grant GR/J88388.

References

Bougeret, J.-L., M. L. Kaiser, P. J. Kellogg, R. Manning, K. Goetz, S. J. Monson, N. Monge, L. Friel, C. A. Meetre, C. Perche, L. Sitruk and S. Hoang, WAVES: The radio and plasma wave investigation on the WIND spacecraft, *Space Sci. Rev.*, 71, 231, 1995.

Cairns, I. H., and D. B. Melrose, A Theory for the $2f_{pe}$ Radiation upstream of the Earth's bow shock, *J. Geophys. Res..*, 90, 6637, 1985.

Cairns, I. H., and P. A. Robinson, Theory for low-frequency modulated Langmuir wave packets, *Geophys. Res. Lett.*, 19, 2187, 1992.

Dudok de Wit, T. and V. V. Krasnosel'skikh, Wavelet bicoherence analysis of strong plasma turbulence at the Earth's quasi-parallel bow shock, *Phys. Plasmas*, 2, 4307, 1995.

Dunckel, N., Low-frequency radio emissions from the Earth and Sun, Ph.D. thesis, Stanford University, 1974.

Elgar, S., Relationships involving third moments and bispectra of a harmonic process, *IEEE Trans. Acoust. Speech. Sig. Proc.*, 12, 1725, 1987.

Ginzburg V. L. and V. V. Zheleznyakov, On the possible mechanisms of sporadic solar radio emission (Radiation in an isotropic plasma), *Soviet Astron.*, 2, 653, 1958.

Goupillaud, P., A. Grossman, and J. Morlet, Cycle-octave and related transforms in seismic signal analysis, *Geoexploration*, 23, 85, 1984.

Gurnett, D. A., The Earth as a radio source: The nonthermal continuum, *J. Geophys. Res..*, 80, 2751, 1975.

Kim Y. C., and E. J. Powers, Digital bispectral analysis and its application to nonlinear wave interactions, *IEEE Trans. Plasma Sci.*, 2, 120, 1979.

Kravtchenko-Berejnoi, V., Analyses polyspectrales et des processus turbulents dans les plasma spatiaux, Ph.D. thesis, University of Orleans, 1994.

Labelle J., and E. J. Lund, Bispectral analysis of equatorial spread F density irregularities, *J. Geophys. Res..*, 97, 8643, 1992.

Lagoutte, D., F. Lefeuvre and J. Hanasz, Application of bicoherence analysis in study of wave interactions in space plasmas, *J. Geophys. Res..*, 94, 435, 1989.

Lagoutte, D., J. C. Cerisier, J. L. Plagnaud, J. P. Villain, and B. Forget, High-latitude ionospheric electrostatic turbulence studied by means of the wavelet transform, *Jour. Atmos. Terr. Phys.*, 54, 1283, 1992.

Melrose, D. B., *Plasma Astrophysics*, Gordon and Breach, New York, 1980.

Papadopoulos, K., M. L. Goldstein, R. A. Smith, Stabilization of electron streams in type III solar radio bursts, *Astrophys. J.*, 190, 175, 1974.

Wild, J., S. F. Smerd, and A. A. Weiss, Solar bursts, *Annu. Rev. Astron. Astrophys.*, 5, 291, 1963.

Yoon, P. H., C. S. Wu, A. F. Vinas, M. J. Reiner, J. Fainberg and R. G. Stone, Theory of $2\omega_{pe}$ radiation induced by the bow shock, *J. Geophys. Res..*, 99, 23,481, 1994.

S. D. Bale and D. Burgess, Astronomy Unit, School of Mathematical Sciences, Queen Mary and Westfield College, Mile End Road, London, E1 4NS, UK (email: S.D.Bale@qmw.ac.uk)

P. J. Kellogg, K. Goetz, R. L. Howard and S. J. Monson, School of Physics and Astronomy, University of Minnesota, Minneapolis, MN, 55455

(received June 19, 1995; revised November 10, 1995; accepted November 15, 1995.)